Proc. Natl. Acad. Sci. USA
Vol. 92, pp. 5910–5914, June 1995
Biochemistry

A catalytic mechanism for the dual-specific phosphatases

JOHN M. DENU AND JACK E. DIXON*

Department of Biological Chemistry, The University of Michigan Medical School, Ann Arbor, MI 48109-0606

Communicated by Minor J. Coon, University of Michigan, Ann Arbor, MI, March 24, 1995 (received for review January 3, 1995)

ABSTRACT **Dual-specific protein-tyrosine phosphatases have the common active-site sequence motif HCXXGXXRS(T). The role of the conserved hydroxyl was investigated by changing serine-131 to an alanine (S131A) in the dual-specific protein-tyrosine phosphatase VHR. The pH profile of the k_{cat}/K_m value for the S131A mutant is indistinguishable from that of the native enzyme. In contrast, the k_{cat} value for S131A mutant is 100-fold lower than that for the native enzyme, and the shape of the pH profile was perturbed from bell-shaped in the native enzyme to a pH-independent curve over the pH range 4.5–9.0. This evidence, along with results from a previous study, suggests that the S131A mutation alters the rate-limiting step in the catalytic mechanism. Formation of a phosphoenzyme intermediate appears to be rate-limiting with the native enzyme, whereas in the S131A mutant breakdown of the intermediate is rate-limiting. This was confirmed by the appearance of a burst of *p*-nitrophenol formation when *p*-nitrophenyl phosphate rapidly reacted with the S131A enzyme in a stopped-flow spectrophotometer. Loss of this hydroxyl group at the active site dramatically diminished the ability of the enzyme to hydrolyze the thiol-phosphate intermediate without exerting any significant change in the steps leading to and including the formation of the intermediate. Consistent with rate-limiting intermediate formation in the native enzyme, the rate of burst in the S131A mutant was 1.5 s^{-1}, which agrees well with the k_{cat} value of 5 s^{-1} observed for native enzyme. The amplitude of the burst was stoichiometric with final enzyme concentration, and the slow linear rate (0.06 s^{-1}) of *p*-nitrophenol formation after the burst was in agreement with the steady-state determined value of k_{cat} (0.055 s^{-1}).**

The dual-specific phosphatases are enzymes capable of dephosphorylating both phosphotyrosine and phosphothreonine/serine residues. The dual-specific phosphatases and the protein-tyrosine phosphatases (PTPases; EC 3.1.3.48) share the active-site sequence motif HCXXGXXRS(T); however, identity outside of this region is limited. The first identified dual-specific phosphatase, VH1, was isolated from the *H1* open reading frame of vaccinia virus (1). Subsequently, Ishibashi *et al.* (2) isolated a dual-specific phosphatase, VHR (for *VH1*-related), from human fibroblasts. Additional dual-specific phosphatases include PAC1 (3) and MKP1 (4), both of which appear to inactivate mitogen-activated protein kinases (ERK-1 or MAP kinase) *in vivo* by direct dephosphorylation of the critical residues Thr-183 and Tyr-185. The *Schizosaccharomyces pombe* enzyme, $p80^{cdc25}$, has also been shown to be a dual-specific phosphatase and is responsible for activating the cyclin-dependent protein kinase $p34^{cdc2}$ by dephosphorylation of Thr-14 and Tyr-15. This dephosphorylation event is required for the cell to enter mitosis (5, 6). Two additional dual-specific phosphatases, YVH1 and MSG5, have been identified in the yeast *Saccharomyces cerevisiae* (7, 8). In the mating pheromone response pathway, MSG5 inactivates FUS3, a MAP kinase homolog.

The publication costs of this article were defrayed in part by page charge payment. This article must therefore be hereby marked "*advertisement*" in accordance with 18 U.S.C. §1734 solely to indicate this fact.

All PTPases and dual-specific phosphatases contain an essential cysteine, which is proposed to be the active-site nucleophile that forms a covalent thiol-phosphate intermediate (9, 10). Activity of VHR toward both phosphotyrosine and phosphoserine/threonine residues is abolished when this catalytic cysteine is replaced with serine, suggesting that both phosphotyrosine and phosphoserine/threonine hydrolysis proceeds via a common active site (10). Although considerable effort has been devoted to understanding the biological function of the dual-specific phosphatases, a detailed understanding of their structure and catalytic mechanism is lacking. Since the dual-specific phosphatase VHR contains only the phosphatase catalytic domain common to all members of this family (11), this enzyme appeared to be an ideal model for exploring the catalytic mechanism.

Using site-directed mutagenesis in conjunction with a detailed kinetic analysis, we have previously shown that the conserved acidic residue Asp-92 in VHR serves as an apparent general acid in the catalytic mechanism (12). In the current study, we explore the function of a conserved hydroxyl group present on Ser-131 within the active site sequence, HCXXGXXRS, using site-directed mutagenesis, chemical modification, pH rate analysis, and rapid-reaction kinetics. We have previously described the kinetics by which VHR dephosphorylates tyrosine and threonine on diphosphorylated peptides corresponding to MAP kinase and JNK1 (11). For the current study, the use of *p*-nitrophenyl phosphate (pNPP) as substrate permits us to carry out the rapid reaction kinetic analysis that is technically impossible with these physiological substrates. We demonstrate that a substitution of Ala for Ser-131 (S131A) had essentially no effect on ligand binding, intermediate formation, or the apparent pK_a of the Cys-124 thiol but dramatically affected the rate of intermediate hydrolysis. When substrate and S131A mutant enzyme were rapidly mixed, a stoichiometric burst of *p*-nitrophenol formation was observed, consistent with rate-limiting hydrolysis of the thiol-phosphate intermediate. The rate-limiting step has been completely converted from intermediate formation in the native enzyme to intermediate breakdown in the S131A mutant. Based on the results presented here, a catalytic mechanism is proposed for the dual-specific phosphatases.

MATERIALS AND METHODS

Materials. All chemicals were of the highest purity commercially available. The native and mutant enzyme were purified to homogeneity as judged by SDS/PAGE. Purification of the S131A enzyme was carried out as described (11).

Site-Directed Mutagenesis. Site-directed mutagenesis was carried out as described (10) using the Bio-Rad Muta-Gene method. The following oligonucleotide was synthesized in an Applied Biosystems model 391 DNA synthesizer and used to construct the S131A mutant: 5′-AGCGTTGGGGCGCGGC-

Abbreviations: PTPase, protein-tyrosine phosphatase; VHR, vaccinia H1 related; pNPP, *p*-nitrophenyl phosphate.

*To whom reprint requests should be addressed at: Department of Biological Chemistry, The University of Michigan Medical School, Room 5416, Medical Science I, Ann Arbor, MI 48109-0606.

TATAAC-3′. The underlined base indicates the change from the naturally occurring nucleotide. The change was verified by DNA sequencing.

Assays. All activity assays were performed using pNPP as substrate as described by Denu *et al.* (11). The buffer was a three-component system consisting of 0.1 M acetate, 0.05 M Tris, and 0.05 M [bis(2-hydroxyethyl)amino]tris(hydroxymethyl)methane (Bistris). This buffer maintains a constant ionic strength of 0.1 M throughout the entire pH range used in these studies (13). To determine the kinetic parameters k_{cat} and k_{cat}/K_m, the initial velocities were measured at various substrate concentrations, and the data were fit to Eq. **1.** For the construction of the pH profiles, k_{cat} and k_{cat}/K_m were determined at various pH values. The pH data were fit to Eqs. **2–4** depending upon the shape of the profile. Data were fit to Eqs. **1** and **2** using the computer programs of Cleland (14) and KINETASYST (IntelliKinetics, State College, PA). Fitting of the pH-dependent data to Eqs. **3** and **4** was accomplished with nonlinear least-squares fitting using NONLIN, a Macintosh version (R. Brenstein, Southern Illinois University) of a computer code developed by Johnson and Frasier (15). In Eqs. **2–4**, C is the pH-independent value of either k_{cat} or k_{cat}/K_m; H is the proton concentration; K_a, K_b, and K_c are the ionization constants of the groups involved in the reaction; and S is the substrate concentration.

$$v = k_{cat}\cdot S/(S + K_m) \quad [1]$$

$$v = C/(1 + H/K_a) \quad [2]$$

$$v = C/[1 + H/K_a)\cdot(1 + K_b/H)] \quad [3]$$

$$v = C/[(1 + H/K_a)\cdot(1 + K_b/H)\cdot(1 + H/K_c)] \quad [4]$$

Inhibition by Phosphate. The inhibition constant for phosphate, K_i, was determined for the S131A mutant enzyme in the following manner. At various fixed concentrations of inhibitor, the initial velocity at different pNPP concentrations was measured as described above. The inhibition was competitive with respect to substrate, and the data were fit using KINETASYST to Eq. **5** to yield the inhibition constant.

$$v = V_{max}\cdot S/(K_m\cdot[1 + I/K_i] + S), \quad [5]$$

where I is the inhibitor concentration.

Inactivation of VHR by Iodoacetate. The pseudo-first-order rate constant for inactivation by iodoacetate was determined using the method described (12).

Rapid-Reaction Kinetics. Enzyme and pNPP were rapidly mixed in an Applied Photophysics stopped-flow spectrophotometer at pH 6 and 30°C. The concentration of pNPP was 1 mM (15-fold higher than the K_m), and the concentrations of VHR were 0.0239, 0.0478, and 0.0942 mM. Enzyme concentration was determined by using an ε_{280} of 11.5 $mM^{-1}\cdot cm^{-1}$ (11) and was verified after dilution by the method of Bradford (Bio-Rad). Product formation (*p*-nitrophenol) was monitored at 405 nm. The data were fit to Eq. **6** using the nonlinear least-squares fitting capability of the kinetics software (Applied Photophysics, Leatherhead, U.K.), where A is the amplitude of the burst, k is the first-order rate of the burst, B is the slope of the linear portion of the curve, C is the intercept of the line, and t is time.

$$\text{Absorbance} = A\cdot e^{(-kt)} + B\cdot t + C \quad [6]$$

The amplitude (in absorbance units) was converted to concentration of *p*-nitrophenol formation at pH 6 using the Henderson–Hasselbach equation, a pK_a value of 7.1, and an ε_{405} of 18 $mM^{-1}\cdot cm^{-1}$. The correlation between the concentration of *p*-nitrophenol burst and final enzyme concentration was determined by linear least-squares fitting.

RESULTS AND DISCUSSION

The rationale for exploring the importance of Ser-131 in VHR was based upon the fact that this residue is either serine or threonine in all PTPases and the dual-specific phosphatases. In addition, the structures of the *Yersinia* PTPase and PTP1B suggested that these hydroxyl residues were within hydrogen-bonding distance of the active-site thiol (16, 17).

Several lines of evidence suggest that the elimination of a conserved hydroxyl group on Ser-131 within the VHR active site sequence motif HCXXGXXRS did not result in an alteration in the overall conformation of the enzyme. The K_i values for binding of the competitive inhibitor, phosphate, were 0.97 mM and 0.65 mM for the native enzyme and S131A mutant, respectively (Table 1). We have also shown that the apparent pK_a value of the active-site cysteine can be determined by monitoring the reactivity of the enzyme with the inactivating agent iodoacetate acid (12). The previously determined pK_a value of Cys-124 in the VHR was 5.61 ± 0.11 (12). The pK_a (Eq. **2**) value determined for the cysteine in the S131A mutant was 5.61 ± 0.18, again suggesting that no major structural difference was detected. It should be noted, however, that the precision of these determinations would not allow us to accurately determine a shift of 0.3 pH unit. Additionally, the chromatographic properties of the mutant enzyme were indistinguishable from those of native protein.

The Effect of pH on the k_{cat}/K_m and k_{cat} Values. The pH dependency of the k_{cat}/K_m value for the S131A mutant was determined and compared to the native enzyme (Fig. 1*A*). The pH dependency of the S131A mutant is identical to that of native enzyme. Both curves ascend with a slope of +2 and descend with a slope of +1, indicating that two ionizable groups must be unprotonated and one group must be protonated for activity (12). We have previously shown (12) that the most likely assignments of the pK_a values for the ascending and descending slopes are as follows: the pK_a of 5.1 appears to correspond to the ionization of the phosphate hydroxyl group present on the substrate, pNPP. The group with a pK_a value of 5.7 is Asp-92 and the group with a pK_a value of 5.47 (5.26–5.71) is the ionization of Cys-124 (12). As in our work with the native enzyme (12), the pK_a values of 5.1 and 5.7 were fixed in fitting the mutant enzyme data to Eq. **4** (See *Materials and Methods* and Table 1). Based on the k_{cat}/K_m pH profile of the mutant enzyme, the pK_a value of Cys-124 is 5.78 (5.61–5.99) (Table 1). Although there appears to be a 0.3 unit increase in the mutant

Table 1. Results of kinetic analysis for native VHR and S131A mutant enzymes

Enzyme	Parameter	Units	Eq.	C	pK_1	pK_2	pK_3
Native	k_{cat}/K_m	$M^{-1}\cdot s^{-1}$	**4**	12.5×10^3 ($0.92–16.2 \times 10^3$)	5.1	5.47 (5.26–5.71)	5.7
S131A mutant	k_{cat}/K_m	$M^{-1}\cdot s^{-1}$	**4**	7.17×10^3 ($5.44–9.18 \times 10^3$)	5.1	5.78 (5.61–5.99)	5.7
Native	k_{cat}	s^{-1}	**3**	7.14 (5.21–9.46)	—	5.26 (5.07–5.48)	7.17 (6.96–7.34)
S131A mutant	k_{cat}	s^{-1}	—	0.058 ± 0.011	—	—	—
Native	K_i	mM	**5**	0.97 ± 0.12	—	—	—
S131A mutant	K_i	mM	**5**	0.65 ± 0.06	—	—	—

Confidence limits of the optimized parameters were determined by using a confidence probability of 67%. The conditions were 0.1 M acetate/0.05 M Tris/0.05 M Bistris at 30°C. C is the pH-independent value of k_{cat} or k_{cat}/K_m.

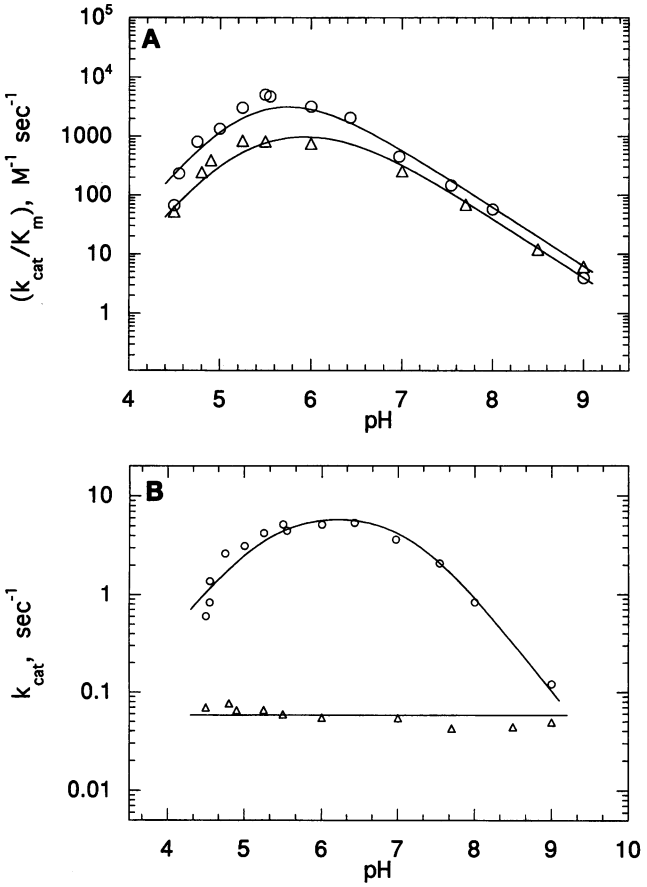

FIG. 1. (*A*) Effect of pH on the k_{cat}/K_m value of the S131A mutant (△) and native enzyme (○). (*B*) Effect of pH on the k_{cat} value of the mutant S131A enzyme (△) and native enzyme (○). The conditions were 0.1 M acetate/0.05 M Tris/0.05 M Bistris at 30°C.

enzyme, the confidence limits (experimental error) indicate that the two values do not significantly differ, but a small perturbation in the pK_a cannot be ruled out. These results suggest that the hydroxyl group of Ser-131 does not play a major role in maintaining the low apparent pK_a of the active site thiol in VHR. The only difference between the curves shown in Fig. 1*A* is a 2- to 4-fold drop in the apparent rate at all pH values. This likely reflects a slight difference in specific activities between the two enzyme preparations and not a significant structural change in the S131A mutant.

The k_{cat} pH profiles of native and S131A enzymes are shown in Fig. 1*B*. The S131A mutant exhibited a >100-fold decrease in k_{cat} (Table 1), and the value was pH independent over the entire pH range investigated. This represents a dramatic difference from the k_{cat} pH profile observed for the native enzyme (Fig. 1*B*). To establish which step in catalysis is altered by the S131A mutation, it is instructive to define the kinetic mechanism and the two kinetic parameters, k_{cat} and k_{cat}/K_m.

Fig. 2 illustrates a minimal kinetic mechanism involving reversible binding of substrate (k_1 and k_2), formation of intermediate (k_3), and intermediate hydrolysis (k_5). A perturbation on k_1 and k_2 by the S131A substitution can be excluded based on the lack of an effect on phosphate binding. Because the K_i value for phosphate inhibition is large and is unaffected in the S131A mutant, it is very likely that phosphate release does not limit k_{cat} in either the mutant or the native enzyme. *p*-Nitrophenol is a very poor inhibitor of PTPases (19), suggesting that dissociation of *p*-nitrophenol from the active site is rapid. Therefore, the dissociation of products (X is *p*-nitrophenol and P is phosphate in Fig. 2) is expected to be rapid and therefore does not influence the kinetic analysis. An

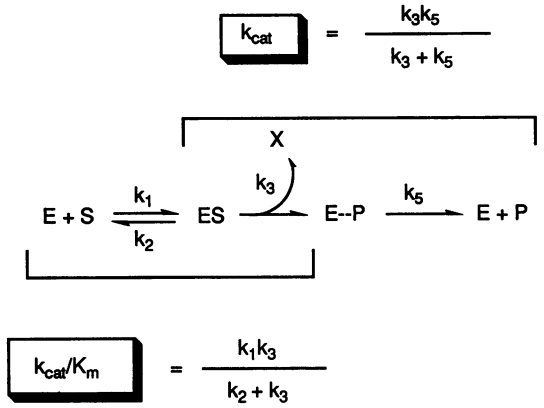

FIG. 2. Kinetic mechanism for VHR. The expressions for the various parameters were determined according to Cleland (18). The rates of the steps were determined as described in *Materials and Methods* and *Results*.

investigation of the k_{cat}/K_m parameter provides information on binding (k_1 and k_2) and intermediate formation (k_3), whereas k_{cat} provides information on both the formation (k_3) and the breakdown (k_5) of the intermediate (Fig. 2). Since there was virtually no effect on the k_{cat}/K_m pH profile, Ser-131 does not play a role in k_3 (intermediate formation). In stark contrast, the k_{cat} value for the S131A mutant is 100-fold slower than the native enzyme and its pH profile is flat throughout the pH range 4.5–9.0, suggesting that the overall rate-determining step has changed. Given the proposed mechanism of Fig. 2, the rate-limiting step in the mutant enzyme is the hydrolysis of the thiol-phosphate intermediate. The absence of any pH dependency indicates that the thiol-phosphate intermediate form of the enzyme, [EP], is inaccessible to bulk solvent (20).

Rapid-Reaction Burst Kinetics. Previous rapid-reaction kinetic experiments with the native enzyme indicated the absence of a burst of *p*-nitrophenol formation (12), suggesting that the slow step in the overall reaction was formation of the intermediate and not its breakdown. The steady-state kinetics of the S131A mutant suggested that intermediate breakdown was reduced to a point in which breakdown became the rate-limiting step in the overall reaction. To test this hypothesis, the S131A enzyme and pNPP were rapidly mixed in a stopped-flow spectrophotometer, and the formation of *p*-nitrophenol was monitored at 405 nm as described in *Materials and Methods*. We predicted that if intermediate hydrolysis was the slowest step in turnover (k_{cat}), a burst of *p*-nitrophenol formation would be observed. As is evident from the data in Fig. 3 there was a burst of *p*-nitrophenol formation followed by a slow linear rate. The amplitude of the burst was stoichiometric with the final enzyme concentration. A stoichiometric burst is anticipated when the relative rate of intermediate hydrolysis is considerably slower than the rate of intermediate formation (21). A less than stoichiometric burst would have been observed if the rate of the slow step (intermediate hydrolysis) was not negligible. The slow linear rate of 0.060 s^{-1} (Fig. 3) is in excellent agreement with the k_{cat} value of 0.055 s^{-1} (S131A mutant) and consistent with rate-limiting intermediate hydrolysis in the S131A mutant enzyme. The exponential rate of the *p*-nitrophenol burst is expected to be the first-order rate constant k_3 for intermediate formation (21). Since we have proposed that the rate-limiting step in k_{cat} for the native enzyme is intermediate formation (12), the value of k_{cat} should agree with the rate of *p*-nitrophenol formation observed in the burst phase of the reaction seen with the S131A mutant. As expected, there is good agreement between these values. The steady-state k_{cat} value for native enzyme is 5 s^{-1}, and the rate of burst formation with the S131A mutant is 1.5 s^{-1}. Given the dramatically different techniques used to

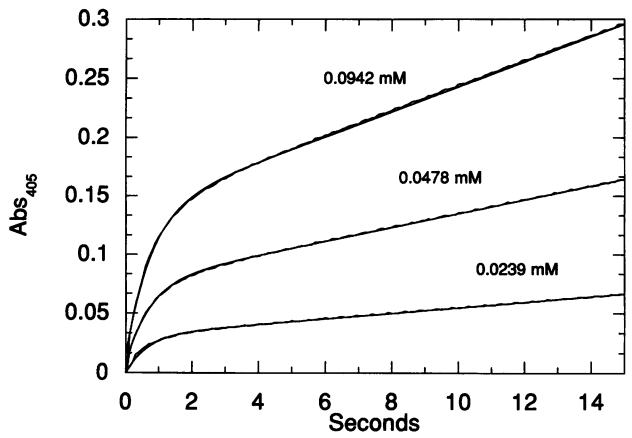

FIG. 3. Rapid-reaction kinetic traces of the S131A mutant enzyme. The numbers listed above each plot refer to the final enzyme concentration. The conditions were 0.1 M acetate/0.05 M Tris/0.05 M Bistris at 30°C. Each data set of 400 points is the average of three determinations, and the solid line is the theoretical fit to Eq. **6**. The amplitude of the burst was directly proportional to the enzyme concentration (0.0239, 0.0478, and 0.0942 mM). The linear correlation between final enzyme *p*-nitrophenol burst concentrations, as described in *Materials and Methods*, yielded a slope of 1.07 ± 0.04 (r^2 = 0.993). The slow linear rate of the kinetic traces was 0.06 ± 0.01 s^{-1}. The rate of *p*-nitrophenol burst was 1.5 ± 0.1 s^{-1} (average) and was independent of enzyme concentration.

measure these rates, it is unlikely that the disparity between 1.5 and 5 s^{-1} represents a significant difference for the rate of intermediate formation (k_3). By using the steady-state and rapid-reaction kinetic constants determined in this study, the rate of intermediate hydrolysis (k_5) for native enzyme was estimated to be at least 50 s^{-1}.

The loss of the hydroxyl in the S131A mutant drastically affects the ability of VHR to hydrolyze the thiol-phosphate intermediate (Fig. 4). Since the pK_a of Cys-124 in the free S131A enzyme is not significantly affected and the k_{cat}/K_m is also virtually unaffected, the interaction between Ser-131 and the thiolate anion (Cys-124) in the Michaelis complex [ES] is not significant. However, in the thiol-phosphate intermediate, [EP], the interaction of Cys-124 and Ser-131 is critical for hydrolysis of the intermediate. Insight into a possible role for this hydroxyl comes from the *Yersinia* PTPase structure, which suggested that the corresponding hydroxyl (Thr-410) is within hydrogen-bonding distance of the catalytic thiol (16). The Ser-131 of VHR could hydrogen bond with Cys-124 in the phosphoenzyme intermediate. Stabilization of the developing negative charge in the transition state of intermediate hydrolysis would make the thiolate a better leaving group (Fig. 4). Alternatively, the inability of alanine (in the S131A mutant) to form this hydrogen bond could alter the conformation or distort the geometry of the phosphoenzyme intermediate in such a way that attack by water is now rate-limiting. In either case, the absence of the hydroxyl would slow intermediate hydrolysis and result in a buildup of the intermediate, as is evident from the results obtained with rapid-reaction kinetics. With the existing data, we cannot discriminate the two potential roles of the conserved hydroxyl. However, the exact function of the conserved hydroxyl may be clearer when the complete three-dimensional structure of VHR is determined.

A Common Catalytic Mechanism for the Dual-Specific Phosphatases. Fig. 4 outlines features of the catalytic mechanism suggested by this study as well as work described previously (12). All PTPases and the dual-specific phosphatases share the active site motif $HC(X)_5RS(T)$, except $p80^{cdc25}$, which does not have the invariant serine/threonine residue. Chemical and mutational evidence suggests that the cysteine (i.e., Cys-124 in Fig. 4) is the active-site nucleophile and is able to form a thiol-phosphate intermediate (10). An invariant acidic residue in the dual-specific phosphatases functions as a general acid, contributing a proton to the phenolate leaving group (12). As is shown in Fig. 4, Asp-92 serves this role in VHR. Formation of the phosphoenzyme intermediate has been observed for the dual-specific phosphatases (10). Rapid kinetic analysis has provided evidence that intermediate formation is the slow step in the catalytic mechanism with the native enzyme, while intermediate breakdown is the slow step in catalysis with the S131A mutant. Breakdown of the phosphoenzyme intermediate is clearly facilitated by Ser-131 of VHR. Hydrolysis of the thiol-phosphate intermediate is expected to be facilitated by a general base, which would activate a water molecule by proton abstraction (Fig. 4). It is attractive to suggest that Asp-92, which protonates the leaving phenolate ion during intermediate formation, might act as the general base during intermediate hydrolysis (Fig. 4). The highly conserved catalytic thiol (Cys-124), general acid (Asp-92), and hydroxyl (Ser-131) residues in the dual-specific phosphatases suggest that most of the enzymes in this family will utilize a common catalytic mechanism.

Similarities in the Catalytic Strategies Employed by the Dual-Specific Phosphatases, PTPases, and Low Molecular Weight Phosphatases. A number of studies suggest that common catalytic strategies are shared by the PTPases and the dual-specific phosphatases. Chemical and mutational evidence suggests that the cysteine is the active-site nucleophile and is able to form a thiol-phosphate intermediate (9, 10, 22). Zhang *et al.* (23) have shown that the invariant R409 residue is critical for substrate recognition and transition-state stabilization. In addition to the conserved active-site sequence motif, there

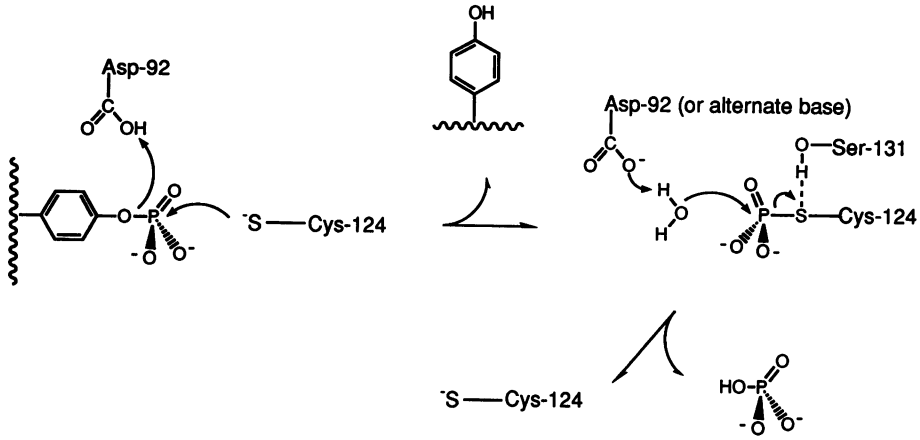

FIG. 4. Common chemical mechanism of PTPases. The numbers refer to the residues found in VHR.

appears to be an important aspartic acid residue that functions as a general acid in the catalytic mechanism of the PTPases (Asp-356 in the *Yersinia* PTPases; refs. 16 and 24). Operationally, Asp-356 in the *Yersinia* PTPase and Asp-92 in VHR both serve as general acids in the catalytic mechanism. In the *Yersinia* enzyme, Asp-356 is found on a flexible loop that, upon ligand binding, undergoes a dramatic conformational change within the protein (16). The loop folds over the active site and brings Asp-356 into a position to act as a general acid. The extraordinary reactivity of the *Yersinia* PTPase has made it difficult to precisely define the rate-limiting step in the catalytic mechanism. For this reason, we want to stress the apparent similarities in residues important for catalysis, but we are hesitant to indicate that these two enzyme families employ identical mechanisms for phosphate monoester hydrolysis.

Another class of phosphatases, originally referred to as low molecular weight acid phosphatases, have also been shown to form a thiol-phosphate intermediate (25). This class of enzymes shares virtually no amino acid sequence identity to the PTPases or dual-specific phosphatases except for a few residues within the active site sequence:

PTPase and dual-specific phosphatase	H	C	X	X	G	X	X	R	S	(T)
Low M_r acid phosphatase	V	C	L	G	N	I	C	R	S	
Consensus sequence	X	C	X	X	X	X	X	R	S	(T)

A comparison of the three-dimensional structure of the PTPases (*Yersinia* PTPase and PTP1B) and the low molecular weight phosphatases revealed no structural identities outside of the active-site sequence, $C(X)_5RS(T)$. The active-site loop forms a phosphate-binding pocket where the phosphate would be positioned between the cysteine and the arginine residues (16, 17, 26, 27). Similar to the PTPases, the low molecular weight acid phosphatases appear to have an important aspartic acid (residue 129), which has been proposed to act as a general acid (26–29). It is interesting that the general features of the catalytic mechanism for phosphate monoester hydrolysis by the PTPases and the low molecular weight phosphatases are similar, yet sequence identity and structural features outside of the active site are clearly distinct. This may represent an example of convergent evolution, where, on more than one occasion, nature has employed similar mechanisms to bring about phosphate monoester hydrolysis.

We thank Dr. Jeff Scholten for the use of the stopped-flow spectrophotometer. We thank Dr. James Peliska for the useful discussions, and we thank Michelle Shukait for her assistance in the preparation of the manuscript. This work was supported by grants from the Walther Cancer Institute and the National Institutes of Health (NIDDKD 18024). J.M.D. holds a National Institutes of Health postdoctoral fellowship (DK07245-17).

1. Guan, K. L. & Dixon, J. E. (1991) *J. Biol. Chem.* **266,** 17026–17030.
2. Ishibashi, T., Bottaro, D. P., Chan, A., Miki, T. & Aaronson, S. A. (1992) *Proc. Natl. Acad. Sci. USA* **89,** 12170–12174.
3. Ward, Y., Gupta, S., Jensen, P., Wartmann, M., Davis, R. J. & Kelly, K. (1994) *Nature (London)* **367,** 651–654.
4. Sun, H., Charles, C. H., Lau, L. F. & Tonks, N. K. (1993) *Cell* **75,** 487–493.
5. Russell, P. & Nurse, P. (1986) *Cell* **45,** 145–153.
6. Gautier, J., Solomon, M. J., Booher, R. N., Bazan, J. F. & Kirschner, M. W. (1991) *Cell* **67,** 197–211.
7. Guan, K., Hakes, D. J., Wang, Y., Park, H.-D., Cooper, T. G. & Dixon, J. E. (1992) *Proc. Natl. Acad. Sci. USA* **89,** 12175–12179.
8. Doi, K., Gartner, A., Ammerer, G., Errede, B., Shinkawa, H., Sugimoto, K. & Matsumoto, K. (1994) *EMBO J.* **13,** 61–70.
9. Guan, K. L. & Dixon, J. E. (1991) *J. Biol. Chem.* **266,** 17026–17030.
10. Zhou, G., Denu, J. M., Wu, L. & Dixon, J. E. (1994) *J. Biol. Chem.* **269,** 28084–28090.
11. Denu, J. M., Zhou, G., Wu, L., Zhoa, R., Yuvaniyama, J., Saper, M. A. & Dixon, J. E. (1995) *J. Biol. Chem.* **270,** 3796–3803.
12. Denu, J. M., Zhou, G., Guo, Y. & Dixon, J. E. (1995) *Biochemistry* **34,** 3396–3403.
13. Ellis, K. J. & Morrison, J. F. (1982) *Methods Enzymol.* **87,** 405–426.
14. Cleland, W. W. (1979) *Methods Enzymol.* **63,** 103–138.
15. Johnson, M. L. & Frasier, S. G. (1985) *Methods Enzymol.* **117,** 301–342.
16. Stuckey, J. E., Schubert, H. L., Fauman, E. B., Zhang, Z.-Y., Dixon, J. E. & Saper, M. A. (1994) *Nature (London)* **370,** 571–575.
17. Barford, D., Flint, A. J. & Tonks, N. K. (1994) *Science* **263,** 1397–1404.
18. Cleland, W. W. (1975) *Biochemistry* **14,** 3220–3224.
19. Zhang, Z.-Y., Malachowski, W. P., Van Etten, R. & Dixon, J. E. (1994) *J. Biol. Chem.* **269,** 8140–8145.
20. Cleland, W. W. (1986) *Investigation of Rates and Mechanisms of Reactions* (Wiley, New York).
21. Fersht, A. (1985) *Enzyme Structure and Mechanism* (Freeman, New York).
22. Cho, H., Krishnaraj, R., Kitas, E., Bannwarth, W., Walsh, C. T. & Anderson, K. S. (1992) *J. Am. Chem. Soc.* **114,** 7296–7298.
23. Zhang, Z.-Y., Wang, Y., Wu, L., Fauman, E., Stuckey, J., Schubert, H., Saper, M. A. & Dixon, J. E. (1994) *Biochemistry* **33,** 15266–15270.
24. Zhang, Z.-Y. & Dixon, J. E. (1994) *Proc. Natl. Acad. Sci. USA* **91,** 1624–1627.
25. Zhang, Z.-Y. & Van Etten, R. L. (1991) *J. Biol. Chem.* **266,** 1516–1525.
26. Su, X.-D., Taddel, N., Stefani, M., Ramponi, G. & Nordlund, P. (1994) *Nature (London)* **370,** 575–578.
27. Zhang, M., Van Etten, R. L. & Stauffacher, C. V. (1994) *Biochemistry* **33,** 11097–11105.
28. Zhang, Z.-T., Harms, E. & Van Etten, R. L. (1994) *J. Biol. Chem.* **269,** 25947–25950.
29. Taddei, N., Chiarugi, P., Cirri, P., Fiaschi, T., Stefani, M., Camici, G., Raugei, G. & Ramponi, G. (1994) *FEBS Lett.* **350,** 328–332.